Proceedings of the ASME 2017 36th International Conference on Ocean, Offshore and Arctic Engineering
OMAE2017
June 25-30, 2017, Trondheim, Norway

OMAE2017-62390

STUDY OF AN ENTRAPPED AIR POCKET DUE TO SLOSHING USING EXPERIMENTS AND NUMERICAL SIMULATIONS

Reza. Firoozkoohi[*]
SINTEF OCEAN [†]
Professor J. H. L. Vogts veg 1,
7052 Trondheim, Norway
reza.firoozkoohi@marintek.sintef.no

Bjørn Christian Abrahamsen
Offshore hydrodynamics
Dept. of Oil and Gas
SINTEF Ocean
Trondheim, Norway

Odd Magnus Faltinsen
AMOS, NTNU[‡]
Trondheim, Norway

ABSTRACT

The capability of the OpenFoam software to model slamming where air is entrapped between the free surface and the structure is investigated. The test case studied is a previously studied phenomenon, where an air pocket is entrapped between the free surface and the upper corner of a rectangular tank during sloshing. The air is entrapped due to the shape of the wave approaching the roof. The air pocket is compressed and starts to oscillate. The oscillations resemble the free oscillations of a mass spring system. OpenFoam results are compared with experiments and a numerical method based on a boundary element method (BEM) both of which are available from the previous study. In this work a compressible VOF (Volume Of Fluid) Eulerian two-phase mixture flow solver called comprssibleInterFoam from OpenFOAM package is used to perform the simulations. The sensitivity of the results to numerical parameters is addressed.

INTRODUCTION

Slamming events accompanied with high pressures impose large local forces on offshore structures and also on the vertical walls of prismatic fuel storage tanks. Free fall of life boats leads to very large pressures as it hits the free surface of the sea water. MARINTEK(Now SINTEF Ocean) has been receiving several projects with focus on slamming events recently. More documentation of the probable forces and pressures is required by classification societies. One phenomenon which often occurs during slamming is associated with entrapped air pocket between the free surface and the structure. The compressible air pocket starts to oscillate, imposing high frequency oscillations on the structure. Abrahamsen [1] studied the oscillation of an air pocket experimentally, numerically and theoretically. Combination of Boundary Element Method (BEM), for the liquid domain, and a lumped model assuming uniform pressure inside the air pocket was used to analyze the oscillating air pocket. The experimental results of this study is used here to validate the numerical results computed by OpenFOAM. Effect of heat exchange on the damping of the oscillating pressure and formation details of the air pocekt can be found in [2]. Tregde [3] also studied the free fall of life boats using Star-CCM+ software. Star-CCM+ uses Finite Volume descritization. It also uses Volume Of Fluid to capture the free surface (same as OpenFOAM). The oscillating air pocket occurs during a flat impact. The CFD simulations capture the oscillation amplitude and frequency with fair agreement with full scale tests. However, full scale tests reveal smaller pressure amplitudes with faster attenuation in time, i.e. larger damping. Lugni et al. [4] studied the evolution of an air cavity due to slamming in a de-pressurized wave impact by extensive experimental work. They divided compression and expansion of the cavity into isotropic and anisotropic stages. In addition, the quick drop in the pressure for which the peak pressure halves within the first two compression/expansion cycles was related to the air leakage

[*]Address all correspondence to this author.
[†]Formerly MARINTEK. SINTEF Ocean from January 1st 2017 through an internal merger in the SINTEF Group
[‡]Center for Autonomous Marine Operations and Systems, Norwegian University of Science and Technology

during closure of the cavity. Similar drop was reported in [1]. It will be shown that OpenFOAM simulations are able to capture this quick drop in pressure.

This study presents modelling of an impact induced air cavity/pocket problem using OpenFOAM. Details of numerical set-up are explained so that the reader can reproduce the same results. The model tests were designed so that a simplest type of bubble would form. By simple we mean that 4 sides of the bubble geometry were determined by the tank wall, i.e. they are flat. In fact these model tests are good candidates for bench marking of numerical codes aiming at modelling compressibility in high pressures.

EXPERIMENTAL SET-UP

The following text is taken from [1] which is the work of second author. Two-dimensional flow was obtained using a slim tank of D=100mm width. The interior length and height of the tank were L=1000mm, Htot=980mm respectively. These dimensions are seen in Fig. 1. The tank was made by 20[mm] thick Plexiglas plates and the filling level H was set to 85% of the tank height (H=0.85Htot) or 0.833m. The tank motion is horizontal.

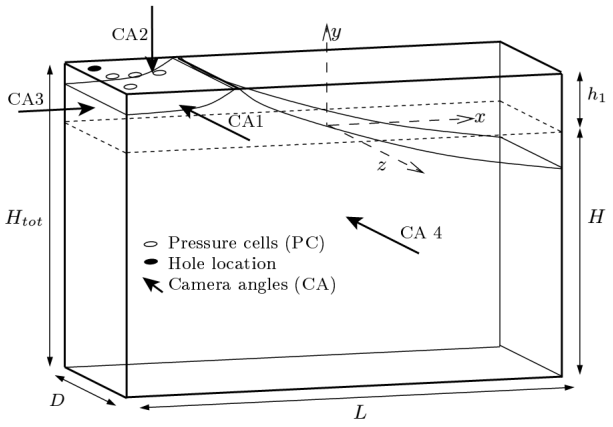

FIGURE 1. A DRAWING OF THE TANK INCLUDING NOTATION FOR DIMENSIONS, CAMERA VIEWS, LOCATION OF THE PRESSURE SENSORS AND DEFINITION OF COORDINATE SYSTEM([1])

In order to get the desired cavity in the experiment, the tank follows a finely tuned motion:

$$\eta(t) = \sum_{i=1}^{i=9} \eta_i(t), \eta_i(t) = \left\{ \begin{array}{c} \eta_i = \eta_{ai} cos(\sigma_i(t - tsi)), t >= t_{si} \\ \eta_i = 0, t < t_{si} \end{array} \right\} \quad (1)$$

Each term in the sum triggers the corresponding natural mode in the tank, because the excitation frequency of each term corresponds to the natural frequency of that mode. Here η_{ai} is the excitation amplitude, t_{si} is the time when the excitation signal i starts. g is gravitational acceleration. σ_i is the natural frequency of the natural modes.

$$\sigma_i = \sqrt{\frac{g\pi i}{l} tanh(\frac{\pi hi}{l})} \quad (2)$$

For the pocket studied here, modes 1, 5 and 9 are used. After some time of exciting modes 5 and 9, they appear as superposed standing waves. Then a signal corresponding to the first mode is added. The time instant t_{si} when the different modes starts is tuned so that the wave hits the roof with an air pocket. The following parameters were chosen to create the pocket: $t_{s1} = 3.820$, $t_{s5} = 0.5652$, $t_{s9} = 0.0$, $\eta_{a1} = 0.202$m, $\eta_{a5} = 0.00145$m and $\eta_{a9} = 0.00077$m.

The experimental excitation system did not exactly reproduce its input signal, so the analytical signal in equation (1) was fitted to the measured position in the experiment and must be considered approximate. For the numerical simulations the acceleration is used directly as input. The resulting pressure time history inside the air pocket is quite repeatable. The latter is true at least for impact events with not too large impact velocity, i.e. less than approximately 0.4m/s.

Horizontal tank position and acceleration are measured and four pressure sensors are attached to the roof at the air cavity. The pressure sensors measure nearly uniform pressure inside the air pocket at a sampling frequency of (9600Hz). The pressure sensor P2 as shown in Fig.2 is used in the next plots. This is located 19mm from the left tank wall (The sensor in the middle).

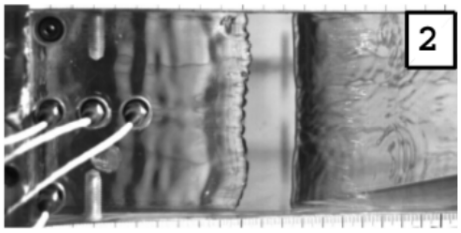

FIGURE 2. FOUR PRESSURE SENSORS USED IN MODEL TESTS.

The pressures measured by all four sensors are shown in Fig.3. This shows that the pressure distribution is quite uniform inside the pocket.

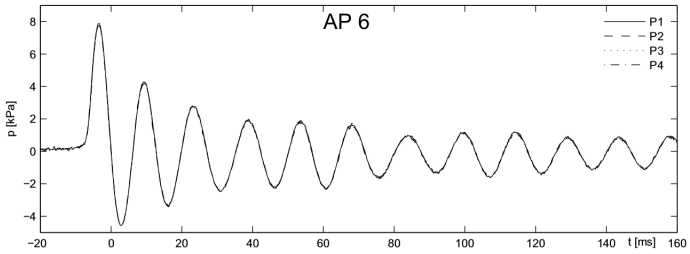

FIGURE 3. MEASURED PRESSURES BY ALL THE 4 PRESSURE SENSORS.

NUMERICAL MODEL and SETUP

Simulations are performed with OpenFOAM which is a free, open source CFD software suitable for research type of work. OpenFOAM uses Finite Volume Method (FVM) for spatial discretization of the flow domain. The version in use is 2.3.1(2.4 also works with the same model). The solver in use is *compressibleInterFoam* that handles non-isothermal compressible two-phase flow of two immiscible fluids. Volume Of Fluid(VOF) method is used for interface capturing. The equations are solved for the two fluids, air and water, handled through volume of fraction of one of the fluids (alpha.water). In our case, water. The latter means the equations are solved simultaneously for the mixture fluid of both air and water.

The simulations were conducted two-dimensionally. No mesh motion is applied and the tank motions are enforced through an additional acceleration term on the right hand side of Navier-Stokes equation. The same method was applied in [5] successfully to study sloshing in a tank with a vertical screen in the middle of the tank. In other words tank-fixed (non-inertial) coordinate system is used. This reduces the computational cost as well when the mesh is large.

Governing Equations

compressibleInterFoam solves continuity, momentum, energy, state and volume of fraction respectively as follows(See [6] and source code in [7]):

$$\frac{\partial \rho}{\partial t} + \nabla \cdot (\rho \mathbf{U}) = 0 \tag{3}$$

$$\frac{\partial (\rho \mathbf{U})}{\partial t} + \nabla \cdot (\rho \mathbf{U}\mathbf{U}) = -\nabla p + \nabla \cdot (\mu \nabla \mathbf{U}) + \mathbf{a} + \mathbf{g} \tag{4}$$

$$\frac{\partial (\rho C_p T)}{\partial t} + \nabla \cdot (\rho \mathbf{U} C_p T) = \nabla \cdot (\kappa \nabla T) \tag{5}$$

$$\rho = \frac{1}{R_a T} p \tag{6}$$

$$\rho = \frac{1}{R_w T} p + \rho_0 \tag{7}$$

$$\frac{\partial \alpha}{\partial t} + \nabla \cdot (\alpha \mathbf{U}) + \nabla \cdot ((1-\alpha)\alpha \mathbf{U}_r) = 0 \tag{8}$$

Bold face variables are vectors. ρ, $\mathbf{U}$, p and T are mixture density, velocity, pressure and temperature. C_p and κ are specific heat and thermal conductivity. $\mathbf{g}$ is the gravitational acceleration vector and $\mathbf{a}$ is the tank acceleration vector. $\mathbf{U}_r$ is the so-called fictitious velocity field used for reducing the thickness of the captured free-surface [8].

Eq. 6 and Eq. 7, are perfect gas and perfect fluid equation of states coupling pressure, temperature and density, for air and water, respectively. R_a and R_w are the universal constants for air and water, 287.058 and 3000, respectively. ρ_0 is the density of water at start time. The description on how the two-phase mixture model is solved in OpenFOAM is given in [8].

Boundary Conditions

Boundary conditions are given in Tab. 1. There is a hole in the roof to mimic the atmospheric pressure of $1e5$ Pascals. The initial temperature is set to 300 Kelvin. Boundary condition *fixedValue* is the equivalent of Dirichlet condition. Zero velocity is applied on all walls except the hole in the roof. *zeroGradient* is equivalent of Neumann condition with a zero-value normal derivative to the boundary. *fixedFluxPressure* is the same as *zeroGradient* but adjusts the normal gradient when body forces such as gravity or surface tension exist. The *pressureInletOutletVelocity* condition specifies *zeroGradient* at all times, except on the tangential component which is set to *fixedValue* for inflow, with the tangential velocity defaulting to 0. *totalPressure* applies a prescribed fixed pressure on the outflow and imposes the dynamic pressure on the prescribed pressure when there is an inflow. *inletOutlet* applies *zeroGradient* if there is an outflow and *fixedValue* in case of inflow. More comprehensive explanation of the boundary conditions can be found in [9].

Numerical Results and Comparison with Model Tests

The free surface profiles at impact moment from both model tests and CFD are shown in Fig. 4. The air pocket is formed at the

TABLE 1. BOUNDARY CONDITIONS. pInletOutletVelocity IS THE SHORTEND FORM OF THE ORIGINAL OPENFOAM BOUNDARY CONDITION NAME pressureInletOutletVelocity.

Field	Walls	Roof hole
U	fixedValue	pInletOutletVelocity
p	calculated	calculated
p_rgh	fixedFluxPressure	totalPressure
T	zeroGradient	inletOutlet
alpha.water	zeroGradient	zeroGradient

top left corner. Close-up images of the air pocket are also shown in Fig. 5. The upper and lower images correspond to maximum and minimum pressures at the initial impact stage. The similarity is good. There are thin jets with three-dimensional structures shooting away from the closing point along the roof. These jets have been captured in the numerical model but somewhat thicker. One needs extremely thin mesh cells to capture these jets. Investigations by Abrahamsen [1] show that the spatial extent of these jets does not have a noticeable effect on the results.

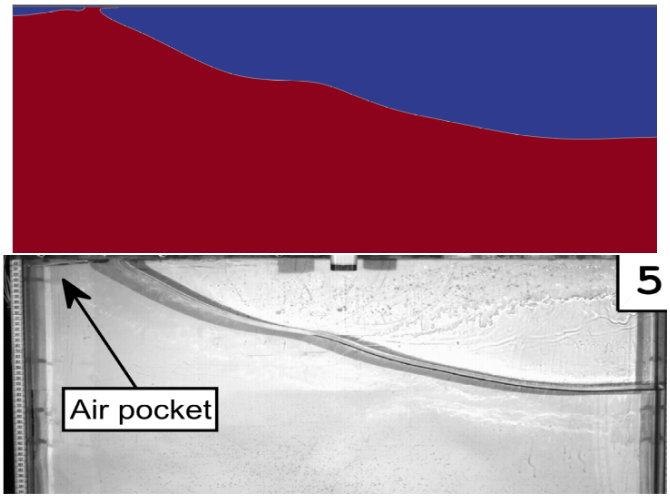

FIGURE 4. FREE SURFACE PROFILE RIGHT AFTER THE IMPACT IN MODEL TESTS AND SIMULATIONS BY OPENFOAM.

Temporal and Spatial Convergence study Temporal and spatial convergence check is performed here by decreasing the Courant number and mesh cell volumes. 5 meshes and 3 Courant number per mesh have been tested. The mesh refinement was done by consecutive division of the background mesh.

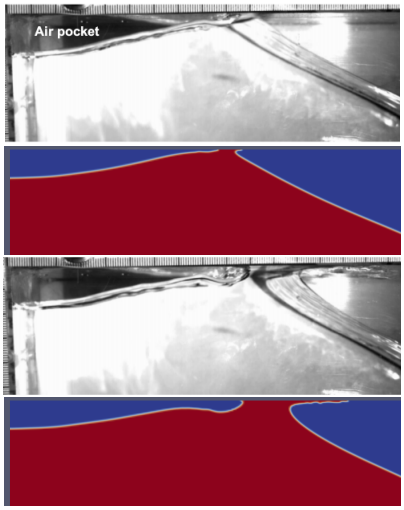

FIGURE 5. FREE SURFACE PROFILE FROM MODEL TESTS AND OPENFOAM, AT THE FIRST MAXIMUM POSITIVE, I.E. THE TWO UPPER SNAPSHOTS, AND MINIMUM PRESSURES, I.E. THE TWO LOWER SNAPSHOTS. THE NUMERICAL RESULTS ARE FOR MESH REFINEMENT LEVEL 4 AND COURANT NUMBER OF 0.2.

The typical mesh used is shown in Fig. 6. The free surface zone is always in a mesh zone where a stronger refinement is applied. The cell size is uniform horizontally and vertically in the refined zone in order to avoid generation of numerical fictitious waves that could affect the shape of the free surface during the impact and eventually the air pocket geometry. The zone from the bottom of the tank up to 0.7m height has a uniform mesh size in horizontal direction but a gradually variable cell height in vertical direction such that when it reaches the refined zone the vertical cell size is almost the same as of the cells in the refined zone. The ratio between the vertical cell size adjacent to the refined zone and the cell size attached to the tank bottom is 0.2.

For temporal convergence analysis, Courant number took values $0.5, 0.3$ and 0.2 (In *OpenFOAM* terminology, *maxCo* and *maxAlphaCo*). Lev**N** in Figs. 7, 8 and 9 expresses that the refined mesh zone was divided **N** times. Lev1 means square cells of 1 cm edge in the refined zone.

Mesh refinement has a clear effect on both the amplitude and period of the oscillations. In fact, it affects the actual size of the pocket by better capturing the pocket boundaries. It also affects the moment for which the air pocket is closed(closure). Smaller time steps, i.e. Courant numbers, also increases the amplitude of the computed pressures for a given mesh. Refining the mesh strongly affects the pressure time history. It is only for refinement levels 4 and higher that pressure oscillations become more similar to model test results. Refinement levels of 5 and 6 well capture the first maxima and minima of the pressures. The os-

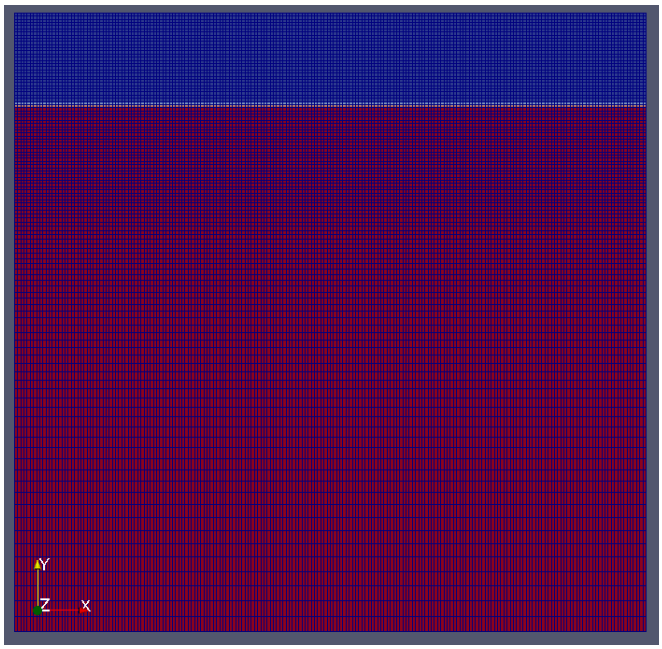

FIGURE 6. MESH USED FOR THE COMPUTATIONS. THE FREE SURFACE ZONE IS IN THE REFINED ZONE. RED AND BLUE COLORS REPRESENT WATER AND AIR, RESPECTIVELY.

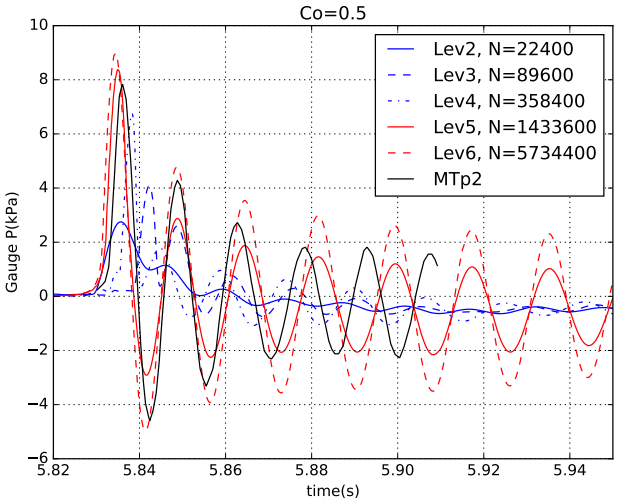

FIGURE 7. SPATIAL AND TEMPORAL CONVERGENCE TESTS OF AIR POCKETS GAUGE PRESSURE AT THE ROOF AND 1CM FROM THE VERTICAL WALL. MTP2 REPRESENTS THE MEASURED PRESSURE AT 2CM FROM THE VERTICAL WALL. THE SECOND PRESSURE SENSOR IN THE MID ROW SHOWN IN Fig. 2. Co=0.5 IN FIGURE TITLE IS THE COURANT NUMBER.

cillation period is also well captured especially for the first three

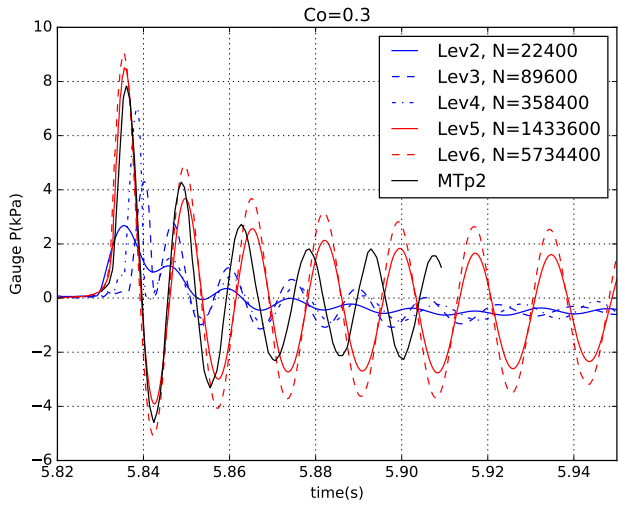

FIGURE 8. CAPTION IS THE SAME AS Fig.7 BUT FOR COURANT NUMBER OF 0.3.

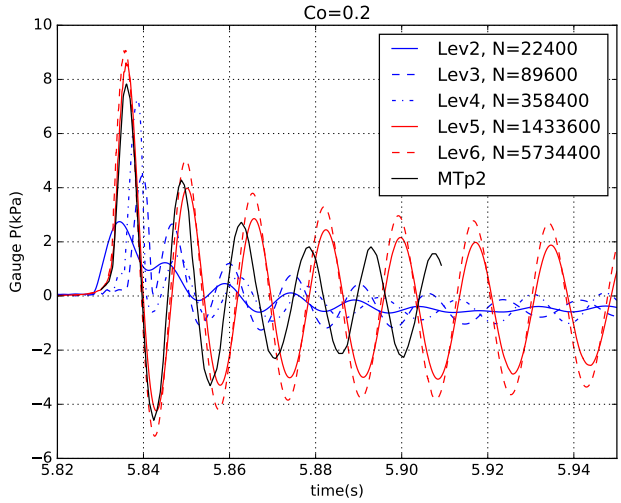

FIGURE 9. CAPTION IS THE SAME AS Fig.7 BUT FOR COURANT NUMBER OF 0.2.

oscillations. The latter shows that the solver in use can be a good candidate for more difficult problems such as an entrapped air pocket on a three dimensional structures.

The variation of consequent periods of the oscillating pocket is shown in Fig.11. The most refined mesh with Lev**6** is chosen. The two numerical methods, CFD and Mixed Eulerian Lagrangian(MEL) from [1], and model tests show that the oscillation period increases for the first consequent oscillations in the selected range, although model test shows a drop after the 3^{rd} period and then increasing again.

The results also show that decreasing the time step, i.e. de-

creasing courant number, improves numerical results in terms of the moment for which the first maxima and minima occur.

The difference in the oscillation period is less than 15% for the mesh with refinement level 6 and the difference in amplitude especially at the initial stage is less than 5%.

The pressure distribution inside the pocket is expected to be uniform as found in model tests. The CFD results also show uniform pressures as shown in Fig. 10.

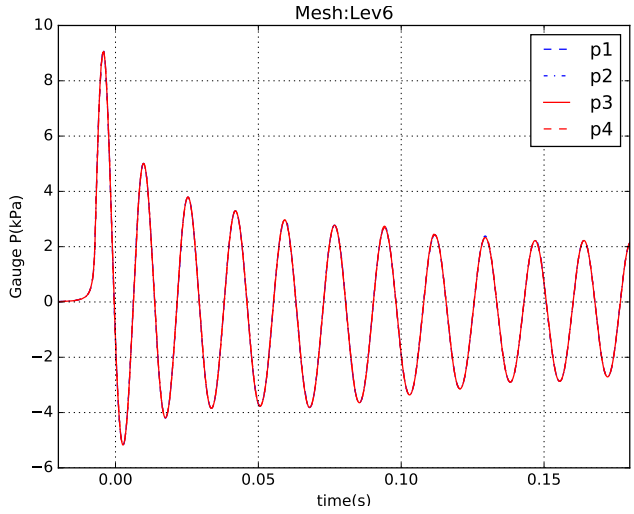

FIGURE 10. COMPUTED PRESSURES BY CFD AT 4 POINTS ON THE ROOF.

The ratio between the first negative and positive peak pressures from model tests is 0.58. This value is 0.57 for mesh refinement of level 6 and Courant number 0.2. For the MEL the ratio was found to be 0.74. [2] concludes that damping of the air pocket oscillations is affected by heat conduction through walls, boundary layer, air leakage and non-linear effects(variable added mass during the pocket oscillations). In the present study, heat transfer through the roof and non-linearities related to local changes in added mass are included but boundary layer is not resolved anywhere. However, we speculate that the reason for good-capturing of the quick drop from the maximum to minimum pressure is related to better capturing the added mass, i.e. the amount of accelerated mass and its acceleration. One could study this speculation by imposing a vertical boundary on the roof close to the closure point to stop the flow extension along the roof away.

The volume of the air pocket at the first maximum and minimum pressures are $\Omega = 82.447 cm^3$ and $\Omega = 95.37 cm^3$, respectively. At the initial stage when the wave crest touches the roof the pocket volume is $\Omega = 86.375 cm^3$. In model tests the initial air pocket volume is estimated to be $\Omega_0 = 81\text{cm}^3$, respectively.

Also in model tests, the average impact velocity along the left wall is estimated to be $V_0 = 0.39$m/s. The vertical velocity of uprising water along a vertical line at 1cm from the vertical wall from below the surface to the free surface is shown in Fig. 12. At the free surface the velocity V_0 is almost 0.3925m/s. This shows that the initial impact velocity is well captured in CFD, for the chosen location. The vertical velocity along the horizontal extent of the pocket and right below it is plotted in 13. The velocity increases along this line for more than 50%.

It is mentioned in [1] that the closing of the pocket occurs by gradually wetting the roof along the width of the tank. The two-dimensional CFD simulations in this study is not able to capture such effect. However this effect does not seem to have a noticeable effect, at least on initial pressures.

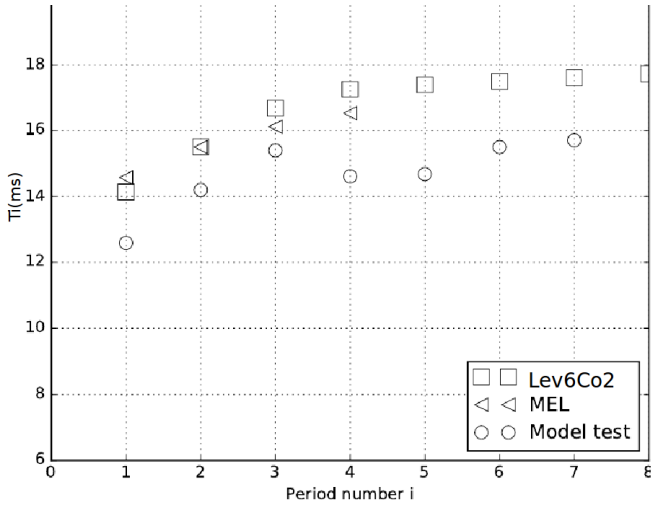

FIGURE 11. VARIATION OF POCKET OSCILLATIONS PERIOD FROM CONSEQUENT OSCILLATIONS. THE VERTICAL AXIS SHOWS THE PRIODS T_i IN MILLISECONDS

HIGH FREQUENCY EFFECTS

The zoom image in Fig.14 shows high frequency small amplitude oscillations superimposed on top of the pocket oscillations. Original and band-passed filtered signals($3000Hz < f < 4500Hz$) are also shown. A closer look Fig.15 shows all the computed pressures. The high frequency oscillations have slightly different amplitudes and periods. The oscillation are not also in phase. Perhaps the varying height of the pocket alnong the roof is the reason for these variations. The results are for mesh level 6 and Courant 0.2. The frequency content of these high pressures is shown in 16. The peak of the energy is around 3850Hz. This high frequency wave might be related to acoustic waves triggered

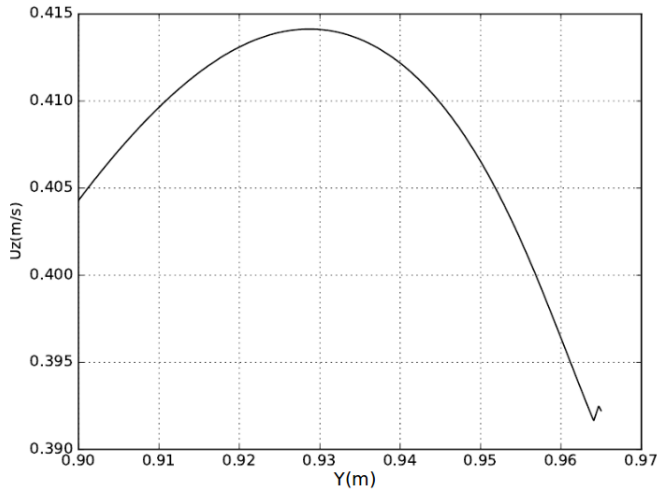

FIGURE 12. VERTICAL VELOCITY COMPONENT OF THE FREE SURFACE TOWARDS THE TANK ROOF AND ALONG A VERTICAL LINE BELOW THE POCKET, AT ONE CM DISTANCE FROM THE VERTICAL WALL, AT IMPACT MOMENT.

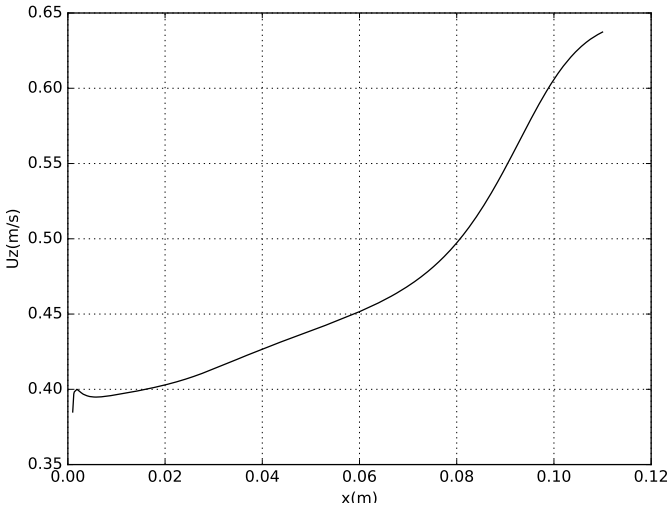

FIGURE 13. VERTICAL VELOCITY COMPONENT OF THE FREE SURFACE TOWARDS THE TANK ROOF AND ALONG HORIZONTAL EXTENT OF THE POCKET AT IMPACT MOMENT.

by the closing of the pocket. The speed of sound, Cs, for a general equation of state may be calculated from 9.

$$C_s = \sqrt{\frac{\partial p}{\partial \rho}} \tag{9}$$

Using the computed data, the speed of sound is found to be 351.8m/s. The average length of the pocket along the roof is about 10cm. Using this info, the lowest acoustic wave has a frequency of 1759Hz. Using the height of the pocket, the lowest frequency (consider p1) is expected to be about 8000Hz. 3850Hz seems to be in between these two limits suggesting that the effective length for standing acoustic waves is somehow between the short and long edges of the pocket. These high frequency waves could not be visible (if exist) in model test results due to low-pass filtering with 1000Hz cut-off frequency. These high frequency oscillations might have numerical reasons. At this stage we are not certain on this matter.

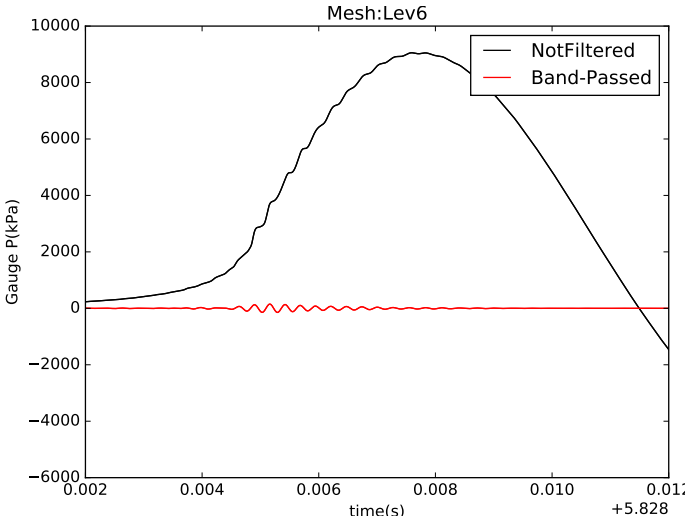

FIGURE 14. NON-FILTERED AND BAND-PASSED SIGNAL WITH CUT-OFF RANGE 3000 HZ$< F <$ 4500 HZ. BOTTOM: FREQUENCY CONTENT OF THE HIGH FREQUENCY PART OF THE SIGNAL

CONCLUDING REMARKS

OepnFOAM (version 2.3.1 or 2.4) was tested for modelling sloshing induced impact problem against model tests. A modest impact event onto the tank roof with an air pocket was selected. 4 boundaries of the air pocket was determined by the tank walls making it a less difficult problem for numerical simulations. The agreement was good in terms of pocket's oscillation frequency but only fair with respect to pressure amplitudes.

The initial impact velocity found by CFD was quite close to those of the model tests assuring that the pre-impact fluid flow was simulated accurately.

Both amplitude and periods of pressure oscillations were well captured by CFD simulations as compared with experi-

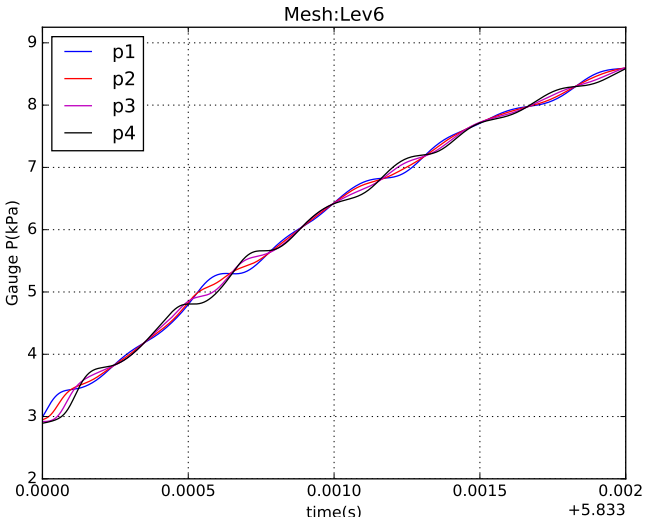

FIGURE 15. ZOOM PLOT OF PRESSURE DURING THE FIRST RISE REVEALING THE HIGH FREQUENCY WAVES

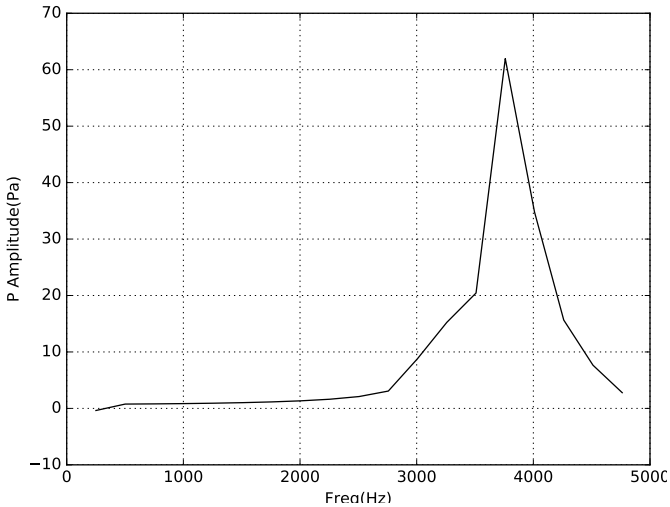

FIGURE 16. FREQUENCY CONTENT OF THE HIGH FREQUENCY PART OF THE SIGNAL

ments. The agreement is very good for the first 3 or 4 oscillation. Later on deviations are noticed for both amplitude and periods.

The sudden drop in the maximum compression pressure to minimum expansion pressure is very well captured. The corresponding ration between these two pressures is 0.58 for model tests and 0.57 with quite close corresponding peak pressures for model tests and CFD simulations. The latter means OpenFOAM is a good candidate for impact problems when compressibility of the lighter phase matter.

High frequency pressure waves superimposed on the air-pocket-related oscillations appeared in the numerical results. Some brief analysis suggested that these waves could not be of acoustic nature. However, we emphasize that more in-depth analysis is required since low-pass filtering of the model test data made it difficult to conclude on the reason for presence of these high frequency waves.

Two-dimensional simulations were used in this study. Model tests show that the closure of the pocket occurs in a three-dimensional manner. The 3D effects should be investigated in the later stage of this study.

Boundary layer was not resolved in this study to reduce the computational cost. The good numerical results suggests that boundary layer effect is not important at least in the initial stage.

REFERENCES

[1] Abrahamsen, B. C., 2011. "Sloshing induced tank-roof impact with entrapped air pocket". PhD Thesis, Norwegian University of Science and Technology, Trondheim, Norway, January.

[2] Abrahamsen, B. C., and Faltinsen, O. M., 2011. "The effect of air leakage and heat exchange on the decay of entrapped air pocket slamming oscillations". *Physics of Fluids,* ***23***(10), p. 102107.

[3] Tregde, V., 2015. "Compressible air effects in cfd simulations of free fall lifeboat drop". Vol. 2, Proceedings of the International Conference on Offshore Mechanics and Arctic Engineering - OMAE.

[4] Lugni, C., Brocchini, M., and Faltinsen, O., 2010. "Evolution of the air cavity during a depressurized wave impact. ii. the dynamic field". *Physics of Fluids,* ***22***(5), May.

[5] Firoozkoohi, R., Faltinsen, O. M., and Arslan, T., 2016. "Investigation of finite water depth sloshing in a tank in the presence of slat screens using model test and cfd". *International Journal of Offshore and Polar Engineering,* ***26***(2), pp. 146 – 153.

[6] Svenungsson, J., 2016. Solving electric field using maxwell's equations and compressibleinterfoamsolver. Web, February. CFD with OpenSource software A course at Chalmers University of Technology.

[7] OpenFOAM-Foundation. C++ source guide. Web. URL:http://cpp.openfoam.org.

[8] Weller, H., 2015. A New Approach to VOF-based Interface Capturing Methods for Incompressible and Compressible Flow. February.

[9] CFDDirect, 2015. Openfoam user guide: 5.2 boundaries. Web, March. URL:http://cfd.direct/openfoam/user-guide/boundaries/.